# Thermo-economic analysis of composite district heating substation with absorption heat pump

Zhangxiang Wu [a, b, 1], Yaran Wang [a, b, 1], Shijun You [a, b], Huan Zhang [a, b], Xuejing Zheng[a, *],Jin Guo[a] , Shen Wei [c]

[a] School of Environmental Science and Engineering, Tianjin University, Tianjin 300350, PR China.

[b] Tianjin Key Lab of Biomass/Wastes Utilization, Tianjin 300350, PR China.

[c] The Bartlett School of Construction and Project Management, University College London(UCL),1-19 Torrington Place, London WC1E7HB, United Kingdom

* Corresponding author: Tel. / Fax: +86 22 2740 0832. E-mail addresses: zhengxuejing@tju.edu.cn.

## ABSTRACT

A novel composite district heating substation (CDHS) with absorption heat pump was proposed and analyzed in this paper. The CDHS was composed of a water-LiBr absorption heat pump and two plate heat exchanges, which could improve the utilization efficiency of geothermal water and the primary supply water of the primary district heating network. The effect of geothermal water temperature and mass flow rate, and primary supply water mass flow rate variation on system performance were investigated and analyzed by case study. The objective was to maximize net profit and minimize payback period by the cascade utilization of the geothermal water and primary supply water. In addition, economic analysis and multi-objective optimization were conducted to find the optimal mass flow rate of the primary supply water based on the TOPSIS decision making method. Exergy loss analysis was applied under the optimal condition to discover which components had the largest exergy loss. Results indicated that, the proposed system had a net profit of 16.22M$ in the life time and the minimum payback period was 2.2 years at the optimal primary supply water mass flow rate of 46.16kg/s where the COP and exergy efficiency of the system were 1.85 and 59.81%, respectively.

[1] These authors contributed equally to this work.

**Keywords**: Geothermal water, Composite district heating system, Absorption heat pump, Economic analysis, Multi-objective optimization

**Nomenclature**

| | |
|---|---|
| $A$ | area ($m^2$) |
| $a$ | solution circulation ratio |
| $c$ | unit cost of exergy ($/kJ) |
| $c_p$ | constant-pressure specific heat of water (kJ/kg/K) |
| $\dot{C}$ | cost rate ($/s) |
| $C_i$ | proximity index |
| $COP$ | coefficient of performance |
| $CRF$ | capital recovery factor |
| $CDHS$ | composite district heating system |
| $D$ | the mass flow rate of working fluid(kg/s) |
| $Ex$ | exergy rate (kW) |
| $EEV$ | electrical expansion valve |
| $F$ | correction factor |
| $h$ | specific enthalpy (kJ/kg) |
| $HP$ | heat price($/GJ) |
| $i$ | annual interest rate(%) |
| $I$ | exergy loss rate(kW) |
| $K$ | overall heat transfer coefficient [$W/(m^2\cdot K)$] |
| $\dot{L}$ | exergy loss rate (kW) |
| $\dot{m}$ | mass flow rate (kg/s) |
| $n$ | system life time (yr) |
| $N$ | annual operating hours (h) |
| $NP$ | net profit ($) |
| $PP$ | payback period (year) |
| $Q$ | heat rate (kW) |
| $s$ | specific entropy [$kJ/(kg\cdot K)$] |
| $S_i^+$ | distance from point i to positive ideal point |
| $S_i^-$ | distance from point i to negative ideal point |
| $t$ | temperature(℃) |
| $T$ | temperature (K) |
| w | concentration of solution(%) |
| $\dot{Z}$ | capital cost rate($/s) |
| $Z$ | capital cost($) |

**Greek letters**

| | |
|---|---|
| $\varphi$ | maintenance factor |
| $\psi$ | exergy efficiency |

**Subscripts**

| | |
|---|---|
| abs | absorber |
| dh | district heating |
| ds | driving source |
| cond | condenser |
| evap | evaporator |
| f | fuel |
| ge | generator |
| gw | geothermal water |
| he | heat exchanger |
| $i$ | ith element |
| in | inlet |
| lm | logarithmic mean |
| out | outlet |
| p | product |
| sol | solution |
| s | supply/strong |
| w | weak |
| ws | weak solution |
| wf | working fluid |

# 1. Introduction

Nowadays, coal, petroleum and other fossil energy have been widely applied in urban district heating (DH), producing a lot of pollutants such as $SO_2$ and $NO_x$. Although switching from coal to natural gas can reduce air pollution, there will be large amounts of greenhouse. Therefore, air pollution and greenhouse gas problems caused by heating are serious in countries with energy structure dominated by fossil fuels in these countries like China [1]. With the rapid decline of fossil energy, the single structure of energy will be greatly impacted by many factors in the future and must be changed. Many researches for renewable energy have been conducted due to several problems caused by fossil fuels, such as pollution, the greenhouse effect and acid rain. Supplying energy via renewable energy is one of the most important methods for environmental protection.

Geothermal energy is reliable, cheap, and environmental-friendly which is a competitive alternative to substitute the conventional fossil fuels. Utilization of the geothermal energy to district heating could be helpful to solve the energy and environmental problems [2]. Due to the limitations of geothermal temperature and equipment investment, most medium-low temperature geothermal source are used for heating [3].Thus, many researchers focus on the utilization of geothermal energy for heating in different patterns. By 2015, there are 82 countries using geothermal energy as heat source for heating [4]. Nian et al. presented a geothermal heating system with abandoned oil wells, and built a heat transfer model. They examined the geothermal production, room temperature and fluid production temperature by the model and indicated that, an abandoned oil well with 3000m depth could be used for heating with the area of 10000m$^2$ [5]. Jonas K et al investigated the exergy and economic performance of a geothermal heat pump aided district heating system. The purpose was to find the optimum solution of the system that the geothermal source was used in a shell and tube type heat exchanger. They found that the system could heat for the number of 13,766 residences and had an attractive investment for Simav region [6].

Miroslav V et al assessed a DH system using geothermal heat pump technology. The environmental sustainability of geothermal heat pumps for district heating were analyzed. The results showed that the geothermal heat pump had the advantages of reducing the inlet primary energy by at least 30% with internal rate of return of up to 38% and payback period of 4.9 years [7].

Absorption heat pump (AHP) is one method for heating because it has large potential to improve energy efficiency, save energy, protect environment and reduce greenhouse gas. Sun et al presented a new configurations of district heating based on natural gas and geothermal energy to reduce gas consumption and irreversible loss. They analyzed the performance of thermodynamic and financial benefit and found that the exergy efficiency could be improved by 12% and the natural gas consumption could be reduced by 54% compared with conventional systems [8]. Lu et al designed a novel gas-fired absorption heat pump that the sensible heat in high-grade and latent heat in low-grade of flue gas were recovered. The pressure of intermediate evaporation and absorption processes could be adjusted to enhance the adaptability in cold regions. The simulated results showed that the energy saving potential of the system could be 39.6% and payback period was 2.5 compared with conventional AHP and gas-fired boiler [9]. Wu et al selected 6 cities with typical climates and the performance of electric driven ground source heat pump and the absorption ground source heat pump were compared and analyzed. The research showed that the efficiency of primary energy utilization and the balance between cold and heat of the absorption ground source heat pump were significantly higher than that of the electric driven ground source heat pump. The difference between them became more and more obvious with the operation of the unit [10].

Both of geothermal energy and AHP contribute a lot for energy saving and environment improvement. Therefore, many efforts have been conducted for theoretical analysis and engineering application. Substantial studies about exergy and economic analysis of AHP are available in open literatures. Luca et al proposed a reversible absorption heat pump and internal combustion engine integration system which employed a water-ammonia mixture. Energy analysis was conducted to evaluate the economic viability and the second-law analysis was applied to compare the system exergy efficiency with conventional systems [11]. Chen et al investigated a proposed compression-absorption heat pump by heat-driven turbine. They built up the mathematical models which included mass conversation, energy conversation and exergy analysis [12]. It can be seen that energy analysis and exergy analysis have been carried out about AHP. In addition, the optimization methods are effective to lower the system cost. Cui et al proposed an innovative cascade absorption heat pump system for recovering low-grade waste heat. They conducted the energy, exergy and economic analyses of the system and optimized total annual cost and exergy destruction by multi-objective optimization method. The results showed that multi-objective optimization scheme was the most comprehensive and optimal scheme of the system [13].

There are numerous studies about the exergy analysis and multi-objective optimization of geothermal water absorption heat pump. However, among district heating technologies, conventional geothermal absorption heat pump has difficulty in fully utilizing geothermal water and primary supply water has poor performance with high return water temperature. For a conventional heating substation in China, return water temperature(60℃-70℃) is too high which can be reduced to improve the energy efficiency. For a conventional geothermal water, it is difficult to recharge water with the temperature below 25℃. There is still a lack of knowledge of CDHS regarding the thermo-economic analysis and multi-objective optimization. Therefore, this paper presented a novel composite district heating substation (CDHS) integrated geothermal water into district heating system which could achieve cascade utilization of geothermal water and improve the utilization efficiency of primary supply water. Then a mathematical model of CDHS in terms of energy, exergy, net profit and payback period was developed to help experiment and engineering design. Further, the payback period and net profit of CDHS was improved through the method of multi-objective optimization. Multi-objective optimization of CDHS was carried out to find the optimal operating condition. Finally, some recommendations were provided for the optimal primary supply water mass flow rate. The main objectives include:

(1)Energy, exergy and economic performance of CDHS should be evaluated.

(2)The optimal mass flow rate of primary supply water of CDHS should be suggested.

(3)The maximum net profit and the minimum payback period should be analyzed.

## 2. System description

The schematic diagram of the CDHS is shown in Fig. 1. The system consists of a water-LiBr absorption heat pump and two plate heat exchangers. There are three cycles including driving source cycle, district heating cycle and the geothermal cycle (illustrated by the red, blue and brown lines, respectively).

For the driving source cycle, primary supply water coming from the DH network is used to drive the absorption heat pump and the heat is delivered to the generator. The medium temperature primary supply water enters the heat exchanger II, to heat the return district water, and the temperature is reduced. The secondary network consists of three branches. In the first branch, the secondary return water passes through absorber and condenser subsequently and absorbs heat. In the second branch, the return district water enters the heat exchanger II and absorbs heat from primary supply water. The secondary return water in the third branch is pumped into exchanger I and the geothermal heat is delivered to it. For the geothermal cycle, the geothermal water(50-70℃) goes through the heat exchanger I and releases heat to district heating water. Then the medium temperature geothermal water (30-40℃) enters the evaporator of the AHP and the temperature is further reduced, and finally it is discharged to the well.

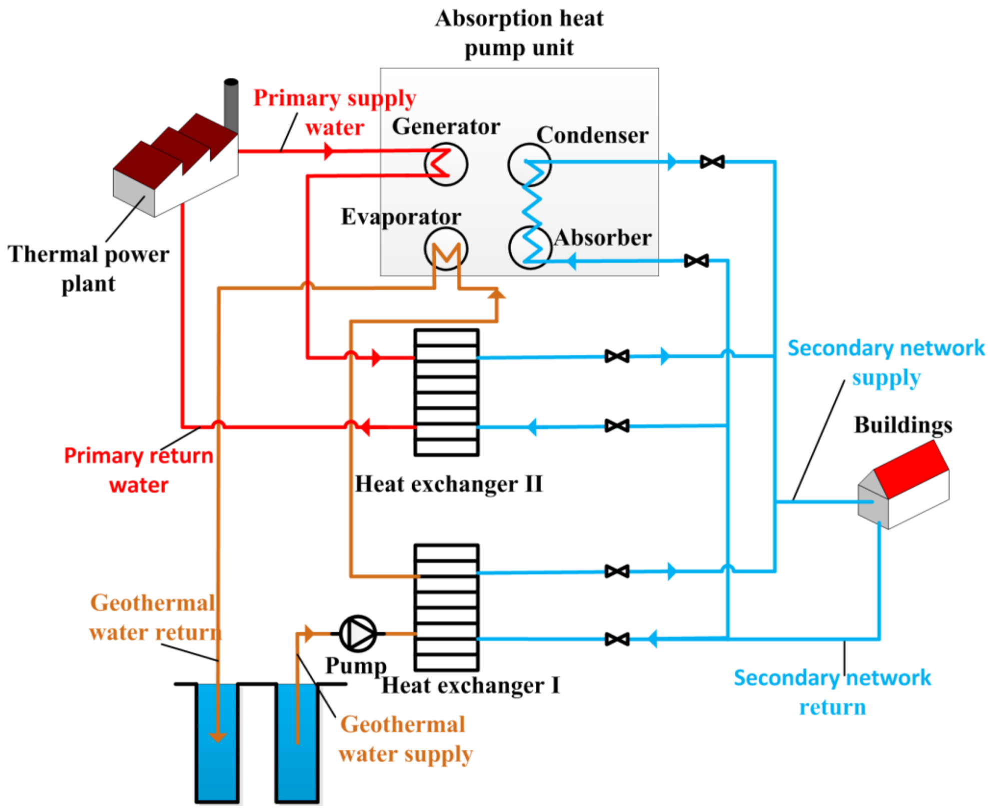


Fig. 1 Schematic diagram of the CDHS

Fig. 2 shows the schematic of AHP which consists of five main sections: evaporator, absorber, condenser, generator and solution heat exchanger. It includes two cycles: solution cycle and working fluid cycle. In the solution cycle, the weak solution from the absorber is pumped into solution heat exchanger. The pressure and concentration remain constant but the temperature increases. Then it enters generator and heated by the primary supply water. As the temperature of the solution rises, vapor is produced and the solution becomes strong solution. The strong solution goes through the solution heat exchanger and flows into the absorber. In the working fluid cycle, the working fluid vapor generating in generator enters condenser and is cooled into liquid. The liquid working fluid is throttled by the EEV and goes into evaporator. The working fluid absorbs heat from the geothermal water in the evaporator and turns into low pressure vapor, and then absorbed by the strong solution in absorber.

The suitable selection of working fluid and solution can reduce cycle thermodynamic inefficiencies and achieve higher energy conversion efficiency and lower capital cost. The solution of LiBr + $H_2O$ was used in absorption cycles around 1930 which had strong hygroscopicity. Water is non-toxic, non-inflammable, in-explosive with large latent heat. LiBr has a high boiling point which is easily soluble in water with stability. Temperature difference of boiling point between $H_2O$ and LiBr ensures the rapidly development of this combination. The efficiency of AHP cycle is higher than the cycle with $NH_3$, but the pressure was lower than that [14]. Therefore, LiBr + $H_2O$ was selected as the working fluid and solution of the absorption heat pump.

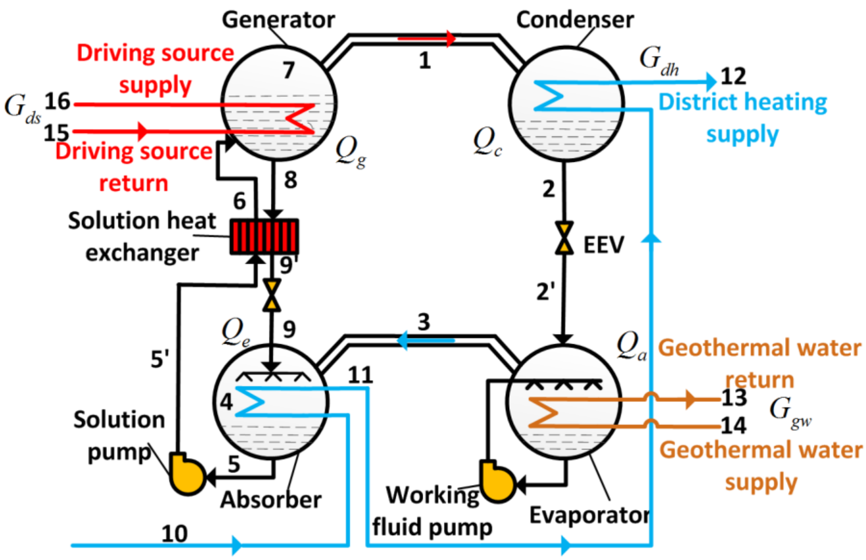


Fig. 2 Schematic diagram of the water-LiBr AHP

## 3. Method

For simplicity, the following assumptions are made during the modeling process:

(1) The system is under state of thermal balance and stable operation, and heat exchange with the environment is neglected.

(2) The working fluid of evaporator and condenser outlet is saturated and reaches the thermal balance.

(3) The working fluid of absorber and generator outlet is saturated solution, and there is no insufficient absorption and insufficient occurrence.

(4) The losses of heat, pressure and flow resistance are ignored.

(5) The enthalpy of the working fluid remains constant before and after the throttling process.

(6) The works of the solution and solvent pumps are neglected.

(7) Logarithmic mean temperature difference is used in heat transfer calculation.

## 3.1. Energy analysis

In the generator and absorber, the energy equation can be formulated as:

$$\begin{cases} Q_{ge.1} = (G_{ws} - D_{wf})h_8 + D_{wf}h_1 - G_{ws}h_6 \\ Q_{abs.1} = (G_{ws} - D_{wf})h_9 + D_{wf}h_3 - G_{ws}h_5 \\ Q_{ge.1} = G_{hs}c_p(t_{15} - t_{16}) \\ Q_{abs.2} = G_{hw}c_p(t_{11} - t_{10}) \end{cases} \tag{1}$$

where $G_{ws}$ is the mass flow rate of weak solution and $D_{wf}$ is the mass flow rate of working fluid. The heat transfer rate of generator can also be expressed as:

$$Q_{ge.1} = D_{wf}[(a-1)h_8 + h_1 - ah_6] \tag{2}$$

where $a$ is solution circulation ratio which can be calculated as:

$$a = \frac{w_s}{w_s - w_w} \tag{3}$$

The energy equation in evaporator and condenser can be defined as：

$$\begin{cases} Q_{cond,1} = D_{wf}(h_1 - h_2) \\ Q_{evap,1} = D_{wf}(h_3 - h_2) \\ Q_{cond,2} = G_{hw}c_p(t_{12} - t_{11}) \\ Q_{evap,2} = G_{gw}c_p(t_{13} - t_{14}) \end{cases} \tag{4}$$

In the solution heat exchanger, the energy equation can be expressed as:

$$Q_{sol,1} = (G_{ws} - D_{wf})(h_8 - h_9) \qquad (5)$$
$$Q_{sol,2} = G_{ws}(h_6 - h_5)$$

The COP of the absorption heat pump is the ratio of the heat capacity to heat consumption and the flowchart is shown in Fig. 3:

$$\text{COP}=\frac{Q}{Q_{ge}}=\frac{Q_{abs}+Q_{cond}}{Q_{ge}}=\frac{Q_{ge}+Q_{evap}}{Q_{ge}} \qquad (6)$$

According to the Eqs(1-6), COP can be expressed as:

$$COP = 1 + \frac{Q_{evap}}{Q_{ge.1}} = 1 + \frac{(a-1)h_8 + h_1 - ah_6}{(h_3 - h_2)} \qquad (7)$$

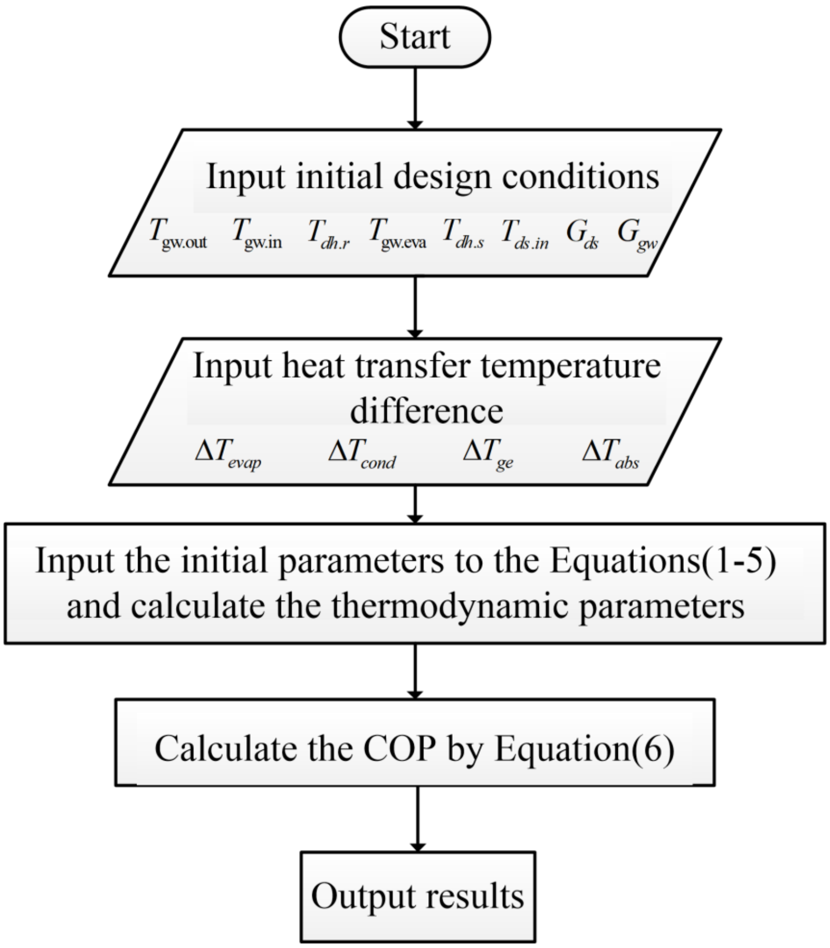

Fig. 3 Flowchart for thermodynamic calculation process.

## 3.2. Exergy analysis

Exergy rate is an effective energy which can be theoretically converted into work. It is made up of physical and chemical exergy when the kinetic and potential energies are ignored. The exergy rate at point i can be calculated as:

$$Ex_i = \dot{m}[(h-h_0)-T_0(s-s_0)] \tag{8}$$

The exergy rate balance equation and the exergy efficiency for each component of the system are given in Table 1.

The performance of the system can be evaluated by the second law of thermodynamics which is based on exergy loss and exergy efficiency. The exergy efficiency of the proposed CDHS can be defined as the ratio of the product exergy rate to the fuel exergy rate [15]:

$$\psi = \frac{Ex_{p,i}}{Ex_{f,i}} \tag{9}$$

In this study, the product and fuel exergy rate can be defined as:

$$Ex_p = Ex_{dh,out} + Ex_{ds,out} \tag{10}$$

$$Ex_f = Ex_{ds,in} + Ex_{gw,in} - Ex_{gw,out} + Ex_{dh,in} \tag{11}$$

Accordingly, the exergy efficiency of the CDHS can be expressed as:

$$\psi = \frac{Ex_{dh,out} + Ex_{ds,out}}{Ex_{ds,in} + Ex_{gw,in} - Ex_{gw,out} + Ex_{dh,in}} \tag{12}$$

Table 1 Exergy rate balance equation and the exergy efficiency for each component

| Component | Exergy balance equation | Exergy efficiency |
|---|---|---|
| Condenser | $Ex_1 + Ex_{11} = Ex_{12} + Ex_2 + I$ | $\psi_{cond} = (Ex_{12} - Ex_{11}) / (Ex_1 - Ex_2)$ |
| Evaporator | $Ex_{13} + Ex_{2'} = Ex_{14} + Ex_3 + I$ | $\psi_{evap} = (Ex_3 - Ex_{2'}) / (Ex_{13} - Ex_{14})$ |
| Absorber | $Ex_9 + Ex_{10} + Ex_3 = Ex_{11} + Ex_5 + I$ | $\psi_{abs} = (Ex_{11} - Ex_{10}) / (Ex_3 + Ex_9 - Ex_5)$ |
| Generator | $Ex_{15} + Ex_6 = Ex_{16} + Ex_1 + Ex_8 + I$ | $\psi_{ge} = (Ex_1 - Ex_6) / (Ex_{15} - Ex_{16} - Ex_8)$ |
| Solution heat exchanger | $Ex_{5'} + Ex_8 = Ex_6 + Ex_{9'} + I$ | $\psi_{sol} = (Ex_6 - Ex_{5'}) / (Ex_8 - Ex_{9'})$ |
| Solution pump | $Ex_5 + W_p = Ex_{5'} + I$ | $\psi_{sp} = (Ex_{5'} - Ex_5) / W_p$ |

## 3.3. Economic model

The economic performance of the proposed CDHS can be evaluated by the unit cost of exergy for the heat capacity which is expressed as:

$$c_{cost} = \frac{\dot{C}_{cost}}{\dot{Q}} \tag{13}$$

where $\dot{C}_{cost}$ is the rate of cost of CDHS. It is the sum of heat source cost rate($\dot{C}_{hs}$) and capital investment and maintenance cost rate($\dot{Z}_k$), and the balance equation is：

$$\dot{C}_{cost} = \dot{C}_{hs} + \dot{Z}_k \tag{14}$$

$$\dot{C}_{hs} = c_{hs}\dot{E}x_{hs.in} \tag{15}$$

$$\dot{Z}_k = \frac{Z_k \times \varphi}{N \times 3600} CRF \tag{16}$$

where $c_{hs}$ is the unit cost of exergy for the heat source. $\varphi$ is the maintenance factor and $N$ is the annual operating hours. $Z_k$ is the capital investment cost of all the components and can be calculated by the equation as follows [16]:

$$Z_k = 1397 \times A_{He}^{0.89} \tag{17}$$

$CRF$ is the capital recovery factor that present value can be converted into a stream of equal annual payments, and it can be described as follows:

$$CRF = \frac{i(1+i)^n}{(1+i)^n - 1} \tag{18}$$

where $i$ is the annual interest rate and $n$ is the system life time.

When calculating $Z_k$, the area of the equipment($A$) must be taken into account and can be expressed as follows:

$$A = \frac{Q}{KF\Delta T_{lm}} \tag{19}$$

Where $K$ and $\Delta T_{lm}$ are the overall heat transfer coefficient and logarithmic mean temperature difference in heat exchangers. F is the LMTD correction factor and can be determined by Fettaka et al [17].

## 3.4. Multi-objective optimization

In this system, the payback period (PP) and net profit (NP) are chosen as objective functions to analyze the thermo-economic performance of the CDHS. The NP is the system life time times the difference of the benefit and cost, and the PP equals to the cost of the system life time divided by the annual benefit. They can be defined as follows:

$$NP = \left(Q \times N \times HP - \dot{C}_{\cos t} \times 3600 \times N\right) \times n \tag{20}$$

$$PP = \frac{\dot{C}_{\cos t} \times 3600 \times n}{Q \times HP} \tag{21}$$

where $HP$ is the heat price.

In this system, it is expected to maximize the NP and minimize the PP, but these two goals are conflict. Therefore, multi-objective optimization is applied to solve this problem. A fuzzy non-dimensionalization method is used to analyze the data of NP and PP, and the TOPSIS method is applied to find the optimal design point in the CDHS [18-21]. The maximizing objective NP and minimizing objective PP can be defined as:

$$NP_i^n = \frac{NP_i - NP_i^{\min}}{NP_i^{\max} - NP_i^{\min}} \tag{22}$$

$$PP_i^n = \frac{PP_i^{\max} - PP_i}{PP_i^{\max} - PP_i^{\min}} \tag{23}$$

where $i$ is the ith element.

TOPSIS method is a multi-objective decision making method. The principal of the method is to define the ideal point and the negative ideal point of the decision making problem which can find the optimal point in the feasible solution. The optimal point is closest to the ideal point and furthest from the negative ideal point. The distance from a point to a positive ideal point($S_i^+$) and the distance to a negative ideal point($S_i^-$) can be expressed as:

$$S_i^+ = \sqrt{(PP_i^n - PP_i^{\max})^2 + (NP_i^n - NP_i^{\max})^2} \tag{24}$$

$$S_i^- = \sqrt{(PP_i^n - PP_i^{\min})^2 + (NP_i^n - NP_i^{\min})^2} \tag{25}$$

The proximity index can be defined as:

$$C_i = \frac{S_i^-}{S_i^+ + S_i^-} \tag{26}$$

If $PP_i$ and $NP_i$ are the ideal solution, then the $C_i$ equals to 1. If they are negative solution, the $C_i$ is equal to 0. The closer $C_i$ gets to 1, the closer the solution is to the ideal solution.

## 4. Case study

In order to ensure the practicability of the system, a commercial center project located in Tianjin (China) is used for performance analysis.There are two geothermal wells. One has an average water production rate of 30kg/s at 60℃ and the other is for recharging. The radiant floor heating is used for space heating in the commercial building, of which the secondary supply and return water temperature are 45℃ and 35 ℃, respectively. Thermodynamic design condition of the system has been listed in Table 2 and the parameters applied in thermo-economic analysis are shown in Table 3.

Table 2 Thermodynamic design conditions of the case.

| Parameters | Value |
|---|---|
| Total heating capacity(MW) | 18 |
| Temperature of the geothermal water outlet, $T_{\mathrm{gw.out}}$ (°C) | 60 |
| Temperature of the geothermal water inlet, $T_{\mathrm{gw.in}}$ (°C) | 19 |
| The temperature of geothermal water at the inlet of evaporator $T_{\mathrm{gw.eva}}$ (°C) | 37 |
| Temperature of the district heating supply water, $T_{dh.s}$ (℃) | 45 |
| Temperature of the district heating return water, $T_{dh.r}$ (℃) | 35 |

| | |
|---|---|
| Temperature of the primary supply water, $T_{ds.in}$ (℃) | 110 |
| Mass flow rate of the primary supply water, $G_{ds}$ (kg/s) | 60 |
| Mass flow rate of the geothermal water, $G_{gw}$ (kg/s) | 30 |
| Temperature difference of evaporator, $\Delta T_{evap}$ (℃) | 2 |
| Temperature difference of condenser, $\Delta T_{cond}$ (℃) | 5 |
| Temperature difference of generator, $\Delta T_{ge}$ (℃) | 3 |
| Temperature difference of absorber, $\Delta T_{abs}$ (℃) | 5 |
| Temperature difference of solution heat exchanger, $\Delta T_{sol}$ (℃) | 20 |
| Overall heat transfer coefficient of the evaporator, $K_{evap}$ [W/(m2 • K)] | 2791 |
| Overall heat transfer coefficient of the condenser, $K_{\mathrm{cond}}$ [W/(m2 • K)] | 5234 |
| Overall heat transfer coefficient of the absorber, $K_{abs}$ [W/(m2 • K)] | 1163 |
| Overall heat transfer coefficient of the generator, $K_{ge}$ [W/(m2 • K)] | 1623 |
| Overall heat transfer coefficient of the solutuion heat exchanger, $K_{sol}$ [W/(m$^2$·K)] | 465 |
| Correction factor of LMTD, $F$ | 1 |
| Ambient temperature, $T_0$ (℃) | 25 |
| Ambient pressure, $p_0$ (kPa) | 101.3 |

Table 3 The parameters using in thermo-economic analysis[22].

| Parameters | Value |
|---|---|
| Annual operational hours, $N$ (h) | 3600 |
| Annual interest rate, $i$ (%) | 14 |
| The system life time, $n$ (year) | 15 |
| Heat price(gas-boiler), $HP$ ($/GJ) | 6.7 |
| Maintenance factor, $\varphi$ | 1.06 |
| Unit cost of exergy for the geothermal source, $c_{hs}$ ( $/GJ) | 6.7 |

## 5. Results and discussion

### 5.1. Performance of the CDHS

The performance of CDHS at variable geothermal water mass flow rate( $G_{gw}$ ) and temperature of geothermal water at the inlet of evaporator( $T_{\mathrm{gw.eva}}$ ) were conducted in this paper.

Fig. 4 shows the variations of the heat capacity and COP with the geothermal water mass flow rate. It can be seen that the heat capacity is almost linearly increased with the increase of geothermal water mass flow rate. But the geothermal water mass flow rate in the range of 20-40kg/s has no impact on the COP. As the geothermal water mass flow rate increases from 20kg/s to 40kg/s, the heat capacity increases from 16.35MW to 19.16MW and the COP remains unchanged, respectively. This can be explained by that the increase of geothermal water mass flow rate leads to the increase of heat transfer in evaporator and exchanger I. Then more vapor generating in evaporator is absorbed which will enhance the absorption capacity and result in the increase of heat capacity. However, operating conditions of the system including temperature, pressure, temperature difference, enthalpy and solution concentration remain unchanged with the increase of geothermal water mass flow rate. According to the Eq(7), COP remains unchanged.

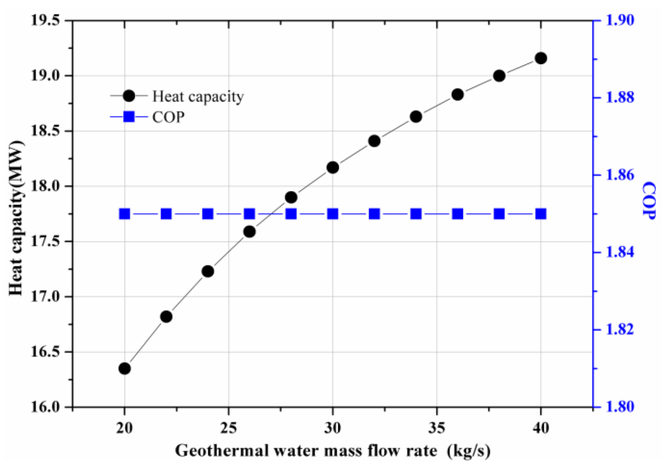

Fig.4 Variation of heat capacity and COP with geothermal water mass flow rate

Fig. 5 displays the tendency of exergy efficiency and unit cost of exergy for heating with geothermal water mass flow rate. What can be seen is that the exergy efficiency and unit cost of exergy for heating decrease with the increase of the geothermal water mass flow rate. According to the Eqs. (8-12), the exergy rate of driving source supply and return water remain unchanged with the increase of geothermal water mass flow rate. The exergy rate of district heating supply and return water, and the exergy rate of geothermal supply and return water rise with the increase of geothermal water mass flow rate. The decrease of exergy efficiency with the increase of geothermal water mass flow rate can be explained by above. Additionally, with the increase of geothermal water mass flow rate, there is an increase in the heat capacity and cost rate. But the growth rate of heat capacity is greater than the cost rate which leads to the decrease of unit cost of exergy for heating. The working fluid changes its phase from liquid to vapor in evaporator.

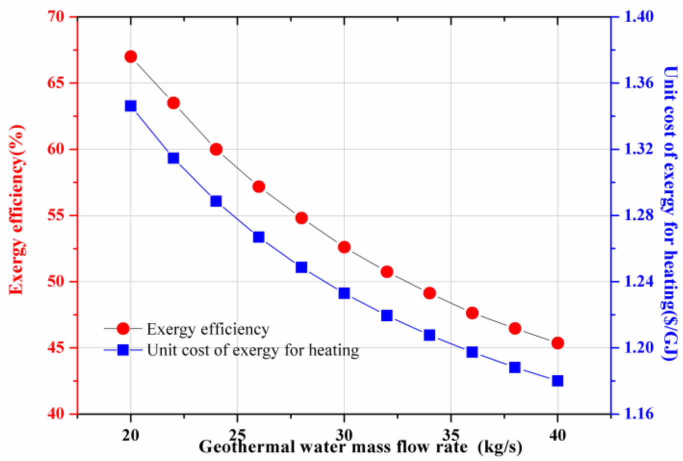


Fig. 5 Variation of exergy efficiency and unit cost of exergy for heating with geothermal water mass flow rate

Figs. 6 and 7 show the effect of the temperature of geothermal water at the inlet of evaporator variation on the system performance. As the temperature of geothermal water at the inlet of evaporator increases from 30℃ to 40℃, the heat capacity increases from 16.36MW to 18.98MW and the COP increases from 1.82 to 1.86. This is because the increase of temperature of geothermal water at the inlet of evaporator results in the increase of solution temperature. Then complete evaporation of working fluid takes place at higher temperature in evaporator and the ability of the solution in the absorber to absorb working fluid vapor is enhanced which causes the increase of heat transfer rate of evaporator. According to the Eq(7), COP is proportional to the heat transfer rate of evaporator. As is shown in the Fig. 7, the exergy efficiency and unit cost of exergy for heating decrease with the increase of temperature of geothermal water into the evaporator.

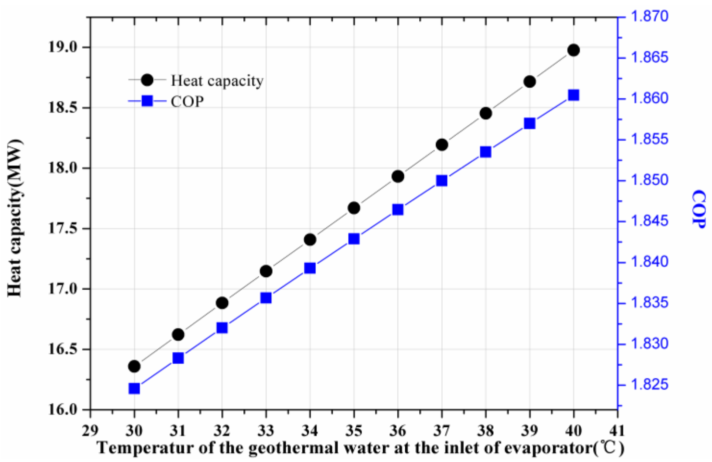


Fig. 6 Variation of heat capacity and COP with the temperature of geothermal water at the inlet of evaporator

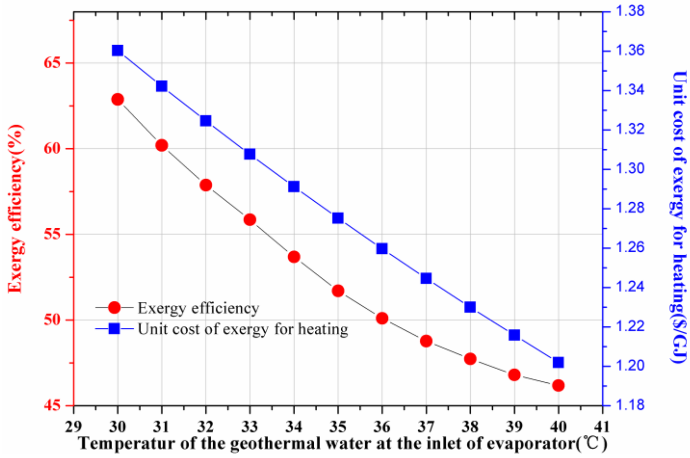


Fig. 7 Variation of exergy efficiency and unit cost of exergy for heating with the temperature of geothermal water at the inlet of evaporator

## 5.2. Optimization analysis

Fig. 8 shows the effect of the primary supply water mass flow rate variation on the system performance. It can be seen that the heat capacity indicates increase as the primary supply water mass flow rate increases. It is obvious that the system has a maximum heat capacity of 18MW and a constant COP of 1.85. Operating conditions of the system remain unchanged with the mass flow rate of the primary supply water. According to the Eq (7), COP remains unchanged. In order to find the optimal mass flow rate of the primary supply water, the multi-objective optimization for the CDHS was conducted.

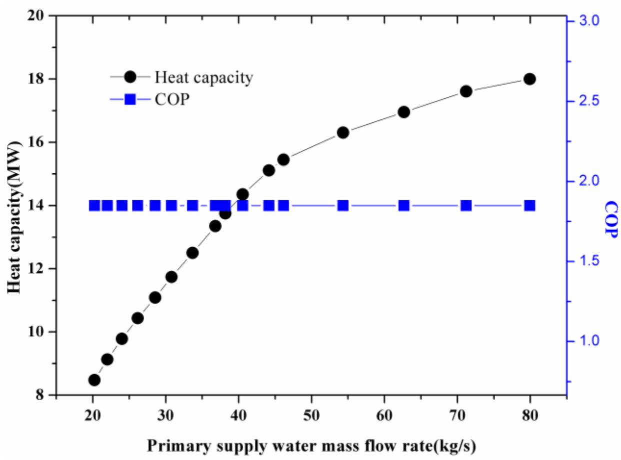

Fig. 8 Variation of heat capacity and COP with the mass flow rate of the primary supply water

Fig. 9 indicates that the net profit increases with the increase of mass flow rate of the primary supply water. However, the payback period shows a trend of falling first and then rising. As the mass flow rate of the primary supply water increases from 20.24kg/s to 79.92kg/s, the net profit increases from 9.22M$ to 17.99M$. The system has a minimum payback period of 2.07 year at the mass flow rate of the primary supply water of 38.17kg/s, where the net profit is 14.68$. The maximum net profit is 19.99M$ at the mass flow rate of the primary supply water is 79.92kg/s, where the payback period is 3.39year.

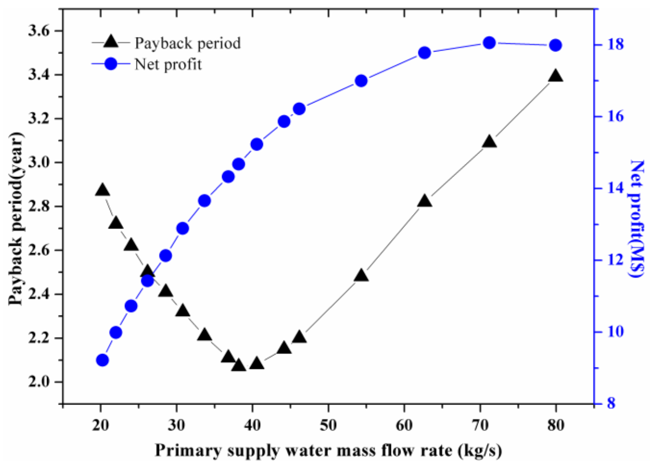


Fig. 9 Variation of payback period and net profit with the mass flow rate of the primary supply water

Fig. 10 shows the relation of non-dimensional net profit and payback period. The TOPSOS decision making method is used to find the optimal design point. It can be seen that the payback period and net profit at optimal point are 2.2year and 16.22M$, where the mass flow rate of the primary supply water is 46.16kg/s and COP is 1.85. Table 4 exhibits the thermodynamic values of the system under the optimal condition.

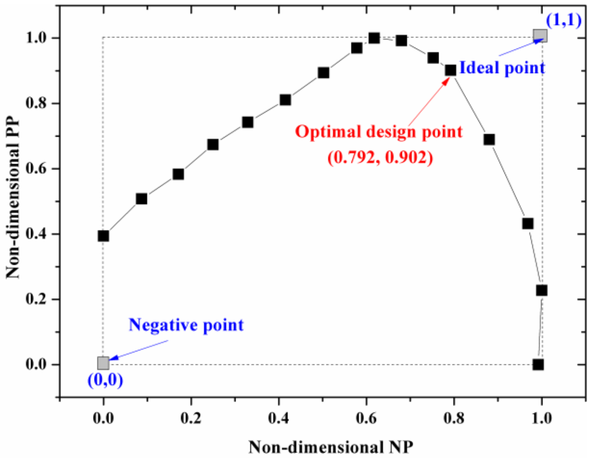


Fig. 10 Non-dimensional payback period and net profit

Table 4 Thermodynamic properties of the system under the optimal condition.

| Parameters | Value |
|---|---|
| Generator heat rate(kW) | 2326.4 |
| Evaporator heat rate(kW) | 1987.7 |
| Condenser heat rate(kW) | 2122.6 |
| Absorber heat rate(kW) | 2192.2 |
| Heat exchanger II heat rate(kW) | 8797.4 |
| Heat exchanger I heat rate(kW) | 2539.8 |
| Working fluid mass flow rate(kg/s) | 0.856 |
| Exergy efficiency | 53% |
| COP | 1.85 |
| Total heating capacity(kW) | 15652.2 |
| Net profit(M$) | 16.22 |
| Payback period(year) | 2.2 |

## 5.3. Exergy loss analysis

The exergy destruction analysis of each component are carried out and shown in Fig. 11 under the optimal condition where the volume of primary supply water is 46.16kg/s. It is necessary to analyze which component has the largest exergy loss. It can be observed that the generator accounts for the biggest amount of the exergy loss which is more than 33%, followed by the solution heat exchanger which is nearly 20%. The evaporator, absorber and condenser have almost the same exergy loss, and the exergy loss of the pump is minimal. This is basically due to that the temperature difference between the primary supply water and working fluid in generator is bigger. Therefore, it is generator that has the biggest potential to decrease the exergy loss of the system and the exergy loss of the generator can be reduced by lowering the temperature difference.

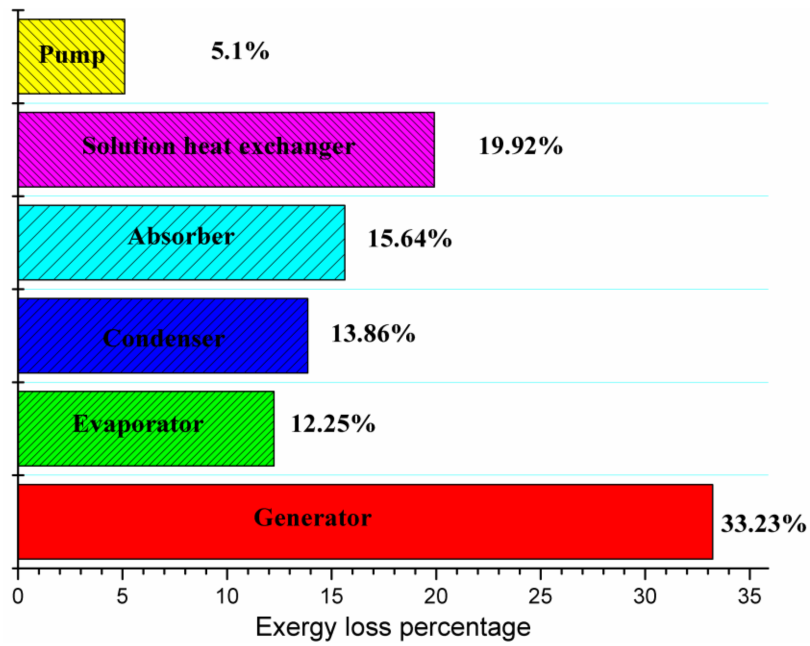


Fig. 11 Exergy destruction percentage of each component under the optimal condition

## 6. Conclusion

In this paper, the performance of a novel composite district heating substation using absorption heat pump based on energy, exergy and economic analysis was carried out. To determine the maximum value of net profit and the minimum value of the payback period, the mass flow rate of the primary supply water were considered. The main conclusions drawn from this paper were summarized as follows:

(1) The heat capacity of the system was mainly influenced by the geothermal water mass flow rate and the temperature of geothermal water at the inlet of evaporator, but they had no effect on the COP. The heat capacity was almost linearly increased with the increase of geothermal water mass flow rate and the temperature of geothermal water at the inlet of evaporator, but the exergy efficiency and unit cost of exergy for heating were opposite.

(2) The optimal primary supply water mass flow rate of the proposed system, based on the TOPSIS decision-making method, was 46.16kg/s for the system under the design conditions.

(3) The system had a net profit of 16.22 M$ in the life time and a small payback period of about 2.2 years under the optimal condition. In addition, COP and exergy efficiency of the system were 1.85 and 59.81%, respectively. The results demonstrated the feasibility and economy of the system.

(4) The generator accounted for the largest share in the total exergy loss, which was due to the large temperature difference between the primary supply water and working fluid.

## Declarations of interest

None

## Acknowledgements

The authors are grateful foe the support provided by the National Key R&D Program of China (No. 2018YFC0705000).


## Reference


[1] Wei W, Baolong W, Tian Y et al. Configurations of solar air source absorption heat pump and comparisons with conventional solar heating. Applied Thermal Engineering 141 (2018) 630-641.

[2] Zhangxiang W, Yufeng Z, Ying S. Energy, exergy, economic(3E) analysis and multi-objective optimization of a novel dual functional integration system. Energy Conversion and Management 199 (2019) 111962.

[3] Jonas K. Jensen, Torben Ommen, Wiebke B. Markussen et al. Design of serially connected district heating heat pumps utilising a geothermal heat source. Energy 137 (2017) 865-877.

[4] Q Zhang, X Zhang, D Sun, et al. Municipal space heating using a ground source absorption heat pump driven by an urban heating system. Geothermics 78 (2019) 224-232.

[5] Yong-Le Nian, Wen-Long Cheng. Evaluation of geothermal heating from abandoned oil wells. Energy 142 (2018) 592-607.

[6] Halit Arat, Oguz Arslan. Exergoeconomic analysis of district heating system boosted by the geothermal heat pump. Energy 119(2017) 1159-1170.

[7] Miroslav V, Aleksandar Si, Vaclav et al. Shallow geothermal energy integration in district heating system: An example from Serbia. Renewable energy 2018.

[8] F Suna, X Zhaoa, X Chena et al. New configurations of district heating system based on natural gas and deep geothermal energy for higher energy efficiency in northern

China. Applied Thermal Engineering 151 (2019) 439-450.

[9] D Lu, G Chen, M Gong et al. Thermodynamic and economic analysis of a gas-fired absorption heat pump for district heating with cascade recovery of flue gas waste heat. Energy Conversion and Management 185 (2019) 87-100.

[10] W Wu, B Wang, T You et al. A potential solution for thermal imbalance of ground source heat pump systems in cold regions: Ground source absorption heat pump. Renewable Energy 59 (2013) 39-48.

[11] L Urbanucci, D Testi. Integration of reversible absorption heat pumps in cogeneration systems: Exergy and economic assessment. Energy Conversion and Management 200 (2019) 112062.

[12] W Chen, ZL Li, Q Sun et al. Energy and exergy analysis of proposed compression-absorption refrigeration assisted by a heat-driven turbine at low evaporating temperature. Energy Conversion and Management 191 (2019) 55-70.

[13] PZ Cui, MX Yu, ZQ Liu et al. Energy, exergy, and economic (3E) analyses and multi-objective optimization of a cascade absorption refrigeration system for low-grade waste heat recovery. Energy Conversion and Management 184 (2019) 249-261.

[14] J Sun, L Fu, S Zhang. A review of working fluids of absorption cycles. Renewable and Sustainable Energy Reviews16 (2012) 1899-1906.

[15] Yunus A. Cengel. Thermodynamics. An Engineering Approach Sixth Edition. Publishing House of Electronics Industry, 2009.

[16] V Jaina, G Sachdeva. Energy, exergy, economic(3E) analyses and multi-objective optimization of vapor absorption heat transformer using NSGA-II technique. Energy Conversion and Management 148 (2017) 1096-1113.

[17] S Fettaka, J Thibault, Y Gupta. Design of shell-and-tube heat exchangers using multiobjective optimization. International Journal of Heat and Mass Transfer 60 (2013) 343-354.

[18] H Sayyaadi, R Mehrabipour. Efficiency enhancement of a gas turbine cycle using an optimized tubular recuperative heat exchanger. Energy 38(2012):362-375.

[19] Xu P, Zhang L, Chen F. Robustness analysis and parameter selection of TOPSIS evaluation model. Renew Stat Decis 2013;17:20-3. Chinese.

[20] M H. Ahmadi, H Sayyaadi, A H. Mohammadi et al. Thermo-economic multi-objective optimization of solar dish-Stirling engine by implementing evolutionary algorithm. Energy Conversion and Management 73 (2013) 370-380.

[21] G Abdollahi, H Sayyaadi. Application of the multi-objective optimization and risk analysis for the sizing of a residential small-scale CCHP system. Energy and Buildings 60 (2013) 330-344.

[22] A Mosaffa, L Farshi, C Ferreira et al. Exergoeconomic and environmental analyses of $CO_2/NH_3$ cascade refrigeration systems equipped with different types of flash tank intercoolers. Energy Conversion and Management 117 (2016) 442-453.